Research on Nanosecond Laser Cleaning Technology of Aerospace Titanium Alloy Oxide Film

Zhichao Li, Qingwen Yun, Donghe Zhang

Abstract—**This manuscript investigates the laser cleaning process of TC1 titanium alloy oxide film spot overlap ratio(*U*) and laser fluence(*F*) as experimental variable. Initial observations revealed that the sample surface was contaminated with oil stains and particulate matter. The oxide film exhibited distinct cleaning stages: partial cleaning, complete cleaning, surface damage, and ridgelike structures with the laser fluence increases when the spot overlap ratio was 70%. Optimal surface quality was achieved at a laser fluence of 6.37 J/cm² and a spot overlap ratio of 70%, and the surface roughness is reduced to about 3.019 μm. Further increases in laser fluence, the roughness continues to decrease, but surface damage, such as microcracks and ridge structure, was also formed on the substrate surface. The laser cleaning had little strengthening effect by analyzing the samples tensile performance before and after laser cleaning. There were fewer surface defects with optimal parameters, and a higher stress and strain cause the specimen fracture. Laser cleaning technology has significant potential for applications in aviation manufacturing and other fields.**

Index Terms—**Titanium Alloy, Laser Cleaning, Surface Morphology, Surface Roughness, Tensile Property.**

I. Introduction

Titanium and its alloys are indispensable light-weight engineering materials with excellent corrosion resistance, high-strength, and good biocompatibility [1-3]. Titanium alloys different grades have been manufactured and widely used in aviation, aerospace, automotive, chemical, medical and other fields [4,5]. However, the titanium chemical properties are relatively active. Titanium and oxygen have a strong reaction tendency at air condition, which has a negative impact on subsequent processing in aviation [6], and must be removed in subsequent processing and production. Traditional cleaning methods include mechanical grinding, chemical cleaning [7,8], and high-pressure water jet cleaning [9]. These technologies often accompany with damaging substrates, polluting the environment, and wasting resources. We need to develop green, efficient, and non-destructive cleaning technology to promote the aviation industry development. Laser cleaning will be an alternative technology for removing oxide film [10]. This method eliminates the need for chemical reagents, and the laser cleaning product is small solid powder, which is easily collected by industrial vacuum cleaners to prevent environmental pollution [11]. Additionally, laser cleaning is a non-contact process, preventing surface stress damage [12]. Laser is pumped from the laser and propagated through optical fibers, and laser can be operated remotely in collaboration with robots. Workers will not work in harsh environment. The cleaning parameters include laser output power, repetition frequency, pulse duration, scanning speed, spot size, and cleaning speed. Multiple pollutants (oxide film, particles, paint and micro-organism) can be removed without or minimizing substrate damaging, and production efficiency can be greatly improved by selecting the optimal cleaning parameters.

Laser cleaning technology has become a popular research direction in recent years. Turner et al. [13-15] respectively used Nd:YAG and CO_2 lasers to clean titanium alloy gas turbine aeroengines, and found that the laser cleaning threshold was 5.98×10^6 W/cm^2. However, surface cracks were observed at higher laser fluence. Whitehead et al. [16] used laser to remove Ti64, Ti6246 and IMI834 titanium alloy oxide film, and the optimal laser cleaning parameter were laser fluence 0.3-0.5 J/cm^2 and 10-100 pulses. The pulse repetition frequency significantly affects the laser cleaning technology. Yue et al. [17] applied nanosecond pulse laser to remove Ti6Al4V α phase layer which was formed at high-temperature, and established the empirical formula to predict α phase layer thickness. Liu et al. [18] applied pulse laser to clean TA15 alloy oxide layer, and investigated the surface morphology. The surface morphology becomes more complex and fails to maintain good surface quality with the laser fluence increases. A remelted layer was formed on the substrate surface. The remelted layer grain was refined by 40%, which strengthened the wear resistance and corrosion resistance. Meanwhile, Liu et al. [19] found that the maximum depth of surface formation gradually increases with the average output power increases. Kumar et al. [20] applied pulsed laser cleaning Ti3Al2.5V titanium alloy tubes, and found that the welded joints had no defects after laser cleaning. The laser cleaning can be used as an alternative process for the welding edges of titanium tubes.

This study employs a nanosecond pulsed laser to clean oxide films from TC1 titanium alloy. Firstly, the laser spot overlap ratio (U) and laser fluence (F) were deduced from

Manuscript received June 10, 2024; revised July 3, 2025.

Zhichao Li is an engineer of Engineering Technology Research Institute, Harbin Hafei Aviation Industry Co., Ltd, Harbin 150080, China (corresponding author to provide phone: +86-451-86582106; e-mail: zhihchaoli1234@163.com).

Qingwen Yun is an engineer of Engineering Technology Research Institute, Harbin Hafei Aviation Industry Co., Ltd, Harbin 150080, China. (e-mail: yqw_1986@163.com).

Donghe. Zhang is an associate professor of Zhengzhou Research Institute Harbin Institute of Technology Zhengzhou, Henan 450000, China. (Another corresponding author, e-mail: zhangdonghe@hit.edu.cn).

different laser parameters so as to reduce the number of laser cleaning process experiments. Secondly, surface morphology and roughness measurements were conducted to determine the optimal laser parameters using a metallographic microscope and a laser confocal microscope. Finally, tensile specimens were prepared for stress-strain experiments to investigate the workpieces mechanical properties, enabling the determination of the optimal laser cleaning parameters.

II. Experimental Scheme

The samples, used in this paper, are TC1 titanium alloy that has been stored for a long time (about 12 months) to form oxide film. The TC1 titanium alloy composition is about Al (1-2.5%), Mn (0.7-2%) and titanium(balance). The large plate was cut into approximately 15×15 cm^2 with a 1 mm thickness. A nanosecond pulsed laser system was employed for the laser cleaning process, and the parameters of the laser cleaning equipment are shown in Table 1. The laser is emitted from the fiber laser and transmitted through the fiber to the collimator. Laser is collimated and expanded into a parallel beam, which is then injected into a two-dimensional scanning mirror through a total reflection mirror. The scanning mirror, driven by motors, enables the laser beam to achieve two-dimensional motion. The laser beams two-dimensional motion was achieved with the mirror swinging action according to reflection relationship. Finally, the beam passes through the F-theta galvanometer and is focused on the focal plane in a certain depth.

The laser experimental parameters were converted into the laser fluence (F), the X-axis spot overlap ratio (U_x) and the Y-axis spot overlap rate (U_y) to simplify the experiments number of according to the parameters relationship. Further simplify the experimental quantity, the overlap ratio of the X-axis and Y-axis is equal (U_x=U_y). The experimental parameters are shown in formulas (1), (2), and (3).

Table 1.
Experimental parameters for laser cleaning

Parameters	Values
Wavelength (nm)	1064
Power (W)	10-1000
Repetition frequency (kHz)	2-50
Pulse duration (ns)	30, 40, 60, 100
Spot diameter (mm)	1
Scanning speed (mm/s)	50-10000
Step distance (μm)	0-10000

$$F = \frac{P}{f \cdot A} \tag{1}$$

$$U_x = \frac{L_x}{D} = \left(1 - \frac{v_s}{D \cdot f}\right) \times 100\% \tag{2}$$

$$U_y = \frac{L_y}{D} \times 100\% \tag{3}$$

Where P is the output power, f is the repetition frequency, t_0 is the laser pulse duration, A is the spot area, L_x is the overlap distance in the x direction, L_y is the overlap distance in the y direction, V_x is the spot scanning speed, and D is the spot diameter.

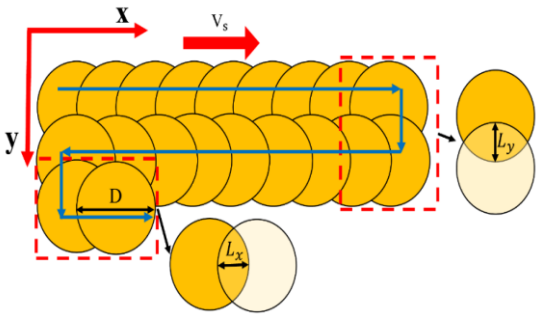

Fig. 1. Laser spots scanning strategy.

A metallographic microscope was used to study the laser cleaning effect. The laser confocal scanning microscopy measured surface roughness. The optimal laser cleaning parameters were obtained with comparing surface ablation and melting states. Tensile tests were conducted on the before and after laser cleaning samples using an electronic universal testing machine, and stress-strain curves were analyzed the laser cleaning influence on samples. A tensile test pieces were shown in the Fig. 2, with a gauge length of 20 mm, a chamfered semicircle radius of 3 mm, and a gauge width of 3.5 mm. The clamping size is 13 mm, and the total length is 52 mm.

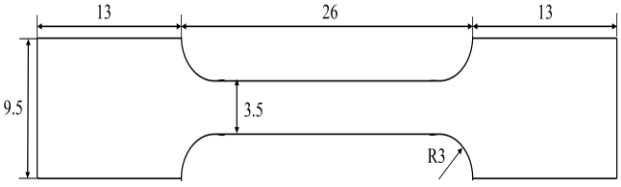

Fig. 2. Tensile specimen size and shape.

III. Results and Discussion

A. Surface morphology

Fig. 3 is the surface topography of the original TC1 titanium alloy. The original oxide film appears silver gray, possibly due to the presence of Ti_2O_3 and TiO_2[21]. The titanium element is oxidized to form anatase-TiO_2 due to sufficient oxygen elements in the air for a long time, anatase-TiO_2 appears gray under reflected light and oxide film appears silver gray. It was found that the scratches were formed on the original sample surface due to longer poor storage. There were discrete black contaminant clusters on the original samples surface in Fig.3 (c).

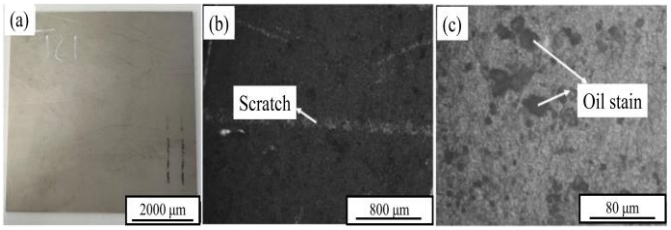

Fig. 3. The morphology of original TC1 titanium alloy. (a) The surface morphology, (b) and (c) micro-morphology with different magnification.

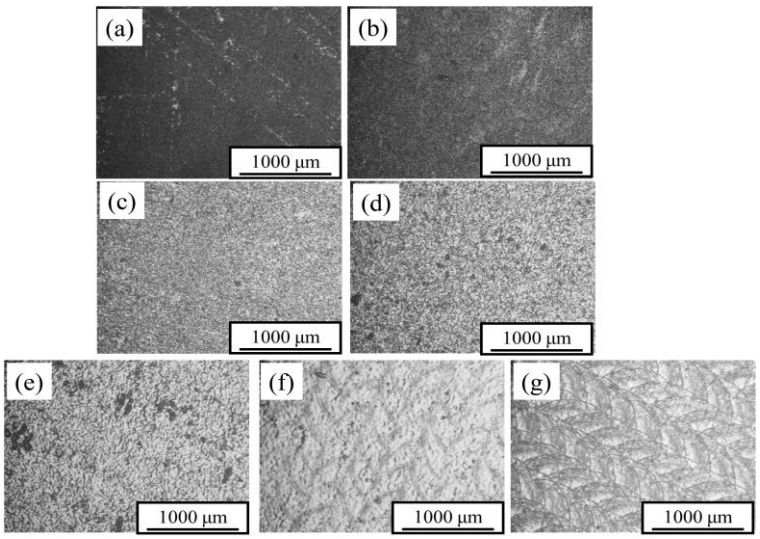

Fig. 4. The micro-morphology with different laser fluence at 80%. (a) 1.27 J/cm^2, (b) 2.55 J/cm^2, (c) 3.82 J/cm^2, (d) 5.10 J/cm^2, (e) 6.37 J/cm^2, (f) 7.64J/cm^2, (g) 8.92 J/cm^2.

Fig.4 shows the surface morphology which was obtained with different laser fluence at spot overlap ratio 80%. The titanium alloy surface morphology will be changed with the laser fluence increases, and the surface oxide film will be gradually removed. The oxide film grayscale has hardly changed when the laser fluence is set to 1.27 J/cm^2. The laser fluence is insufficient, and the oxide film does not melt. The oxide film was not removed. The oxide film has been melted when the laser fluence reaches 2.55 J/cm^2, and the surface gray-scale gradually decreases. When the laser fluence exceeds 3.82 J/cm^2, the oxide film is completely removed, and the surface black completely disappears. The surface gray-scale becomes bright, and the surface morphology is poor for many ripples generated with melting substrate and solidification. Finally, the laser fluence increased to 7.64 J/cm^2, and periodic micro nano-structures were formed on the surface. The surface micros-structure was strengthened with the laser fluence continues to increase. The optimal surface morphology was not achieving with spot overlap ratio 80%. The oxide film will be melted with higher fluence. The melting depth also increases when the laser fluence is beyond 7.64 J/cm^2. A microscopic morphology will be formed by laser shock after solidification. The spot continuously overlaps and manufactures the periodic structure during laser cleaning, resulting in poor surface morphology.

Fig. 5 presents the surface morphology with a spot overlap ratio 70%. There is a small fluctuation on the surface when the laser fluence is 1.27 J/cm^2, and the surface change is not significant. Only oil and grease are removed, and the oxide film is partially removed, while the surface maintains original state. When the laser fluence is 2.55 J/cm^2, the smaller fluctuations were reduced for oxide film remelting solidification, and original large raised structure was retained. The oxide film was partially removed and becomes smoother, and the molten oxide film cools rapidly due to the low laser fluence, ultimately forming lager ripple structure. When the laser fluence is between 5.10 J/cm^2 and 6.37 J/cm^2, the surface ripple structure almost disappears and the surface quality is best. When the laser fluence exceeded 7.64 J/cm^2, a ridge structure is formed on the surface due to the effects of laser shock, plasma, gravity and molten substrate surface tension, and this micros-structure has potential for future applications. In summary, the surface quality is optimal when the laser fluence is 5.10- 6.37 J/cm^2.

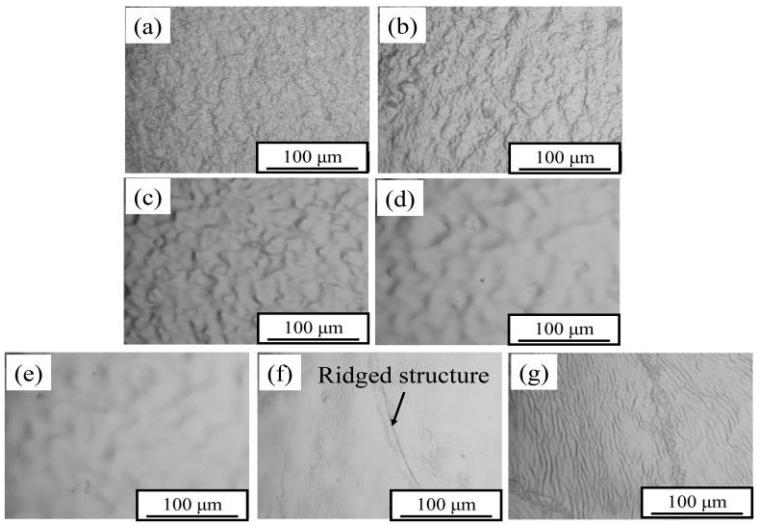

Fig. 5. The micro-morphology with different laser fluence at 70%. (a) 1.27 J/cm^2, (b) 2.55 J/cm^2, (c) 3.82 J/cm^2, (d) 5.10 J/cm^2, (e) 6.37 J/cm^2, (f) 7.64J/cm^2, (g) 8.92 J/cm^2.

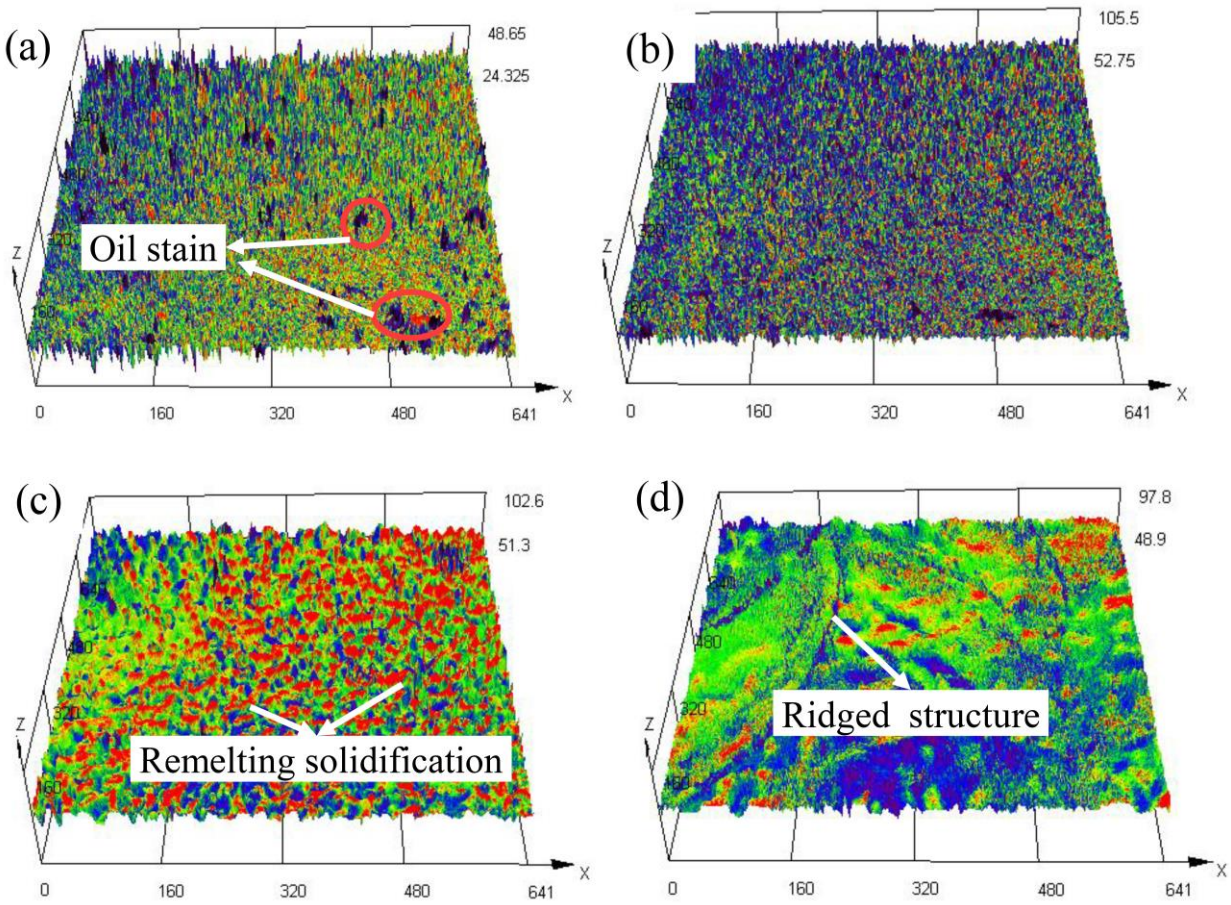

Fig. 6. The 3D morphology with different laser fluence at 70%. (a) 1.27 J/cm^2, (b) 3.82 J/cm^2, (c) 6.37 J/cm^2, (d) 7.64 J/cm^2.

B. Roughness analysis

Fig. 6 shows 3D morphology with different laser fluence at 70%. The black aggregates can be seen in Fig. 6(a), presenting pollutants such as oil stains on the surface. Oil stains are significantly removed when the laser fluence is 1.27 J/cm^2, and the black aggregates decrease or disappear. When the laser fluence reaches 3.82 J/cm^2, the melting and solidification marks appeared on the oxide film surface. The surface oxide film is completely removed at 6.37 J/cm^2, and the melting and solidification marks decreased. The surface quality was best. When the laser fluence continues to exceed 7.64 J/cm^2, the surface presents a ridge structure, and the substrate was damaged.

Fig. 7 shows the surface roughness with different laser fluence at 70%. The surface roughness first increases and then decreases with laser fluence increases. There are oil stains on the original sample surface, and the roughness is moderation about 3.25 μm. The surface oil stain is completely removed with increase laser fluence by heating and evaporation. However, the laser fluence failed to remove the oxide film at 1.27 J/cm^2, and the roughness increase to 4.38 μm. Continuing to increase the laser fluence to 2.55 J/cm^2, the oxide film shows a remelted and solidified state, and the surface roughness decreases. But the ripples appear on the surface and the roughness slightly increases with 3.82 J/cm^2. The laser fluence continues to increase, and the surface morphology and flatness will increase. The surface will gradually become smoother and the roughness will gradually decrease. The roughness is approximately 3.02 μm with laser fluence of 6.37 J/cm^2.

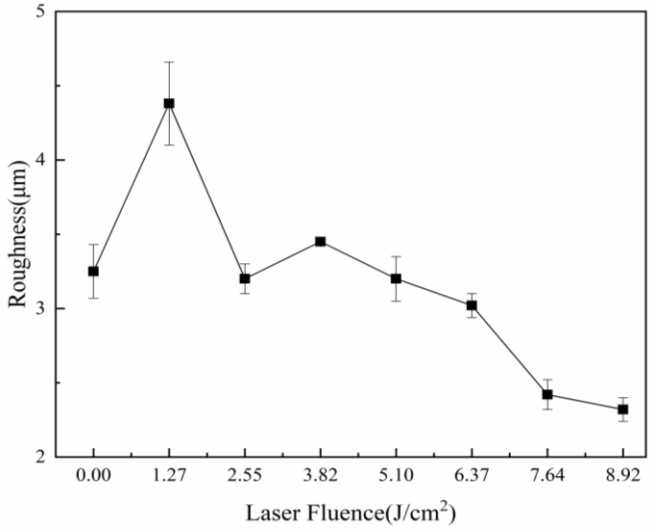

Fig. 7. Surface roughness with different laser fluence at 70%.

C. Mechanical properties

The standard samples were prepared and subjected to tensile testing to study the influence of laser cleaning effect on mechanical properties. Fig. 8 is the stress-strain curves with different laser fluence at 70%. The removal effect on titanium alloy specimens is not significant. The main reason is that the surface melting and heat affected layer are only small at the micrometer level with nanosecond pulse laser according to the previous research results [22], which is negligible compared to the thickness of the specimen at the millimeter level, so the material mechanical properties is

relatively small. However, there are fewer surface defects at 6.37 J/cm^2 (Fig. 5 (e)), and the tensile specimen is less prone to microcracks and stress concentration during the elongation process. The original sample, laser partial cleaning, and surface damage have many surface defects, and microcracks are generated during the stretching process. Microcracks will become stress concentration points, and will further expand, making the sample more prone to fracture. Besides, the surface layer will take place fine crystal strengthening during laser cleaning [17]. So, the stress and strain were maximum about 647 MPa and 26% with laser fluence 6.37 J/cm^2 and spot overlap ratio 70%, respectively.

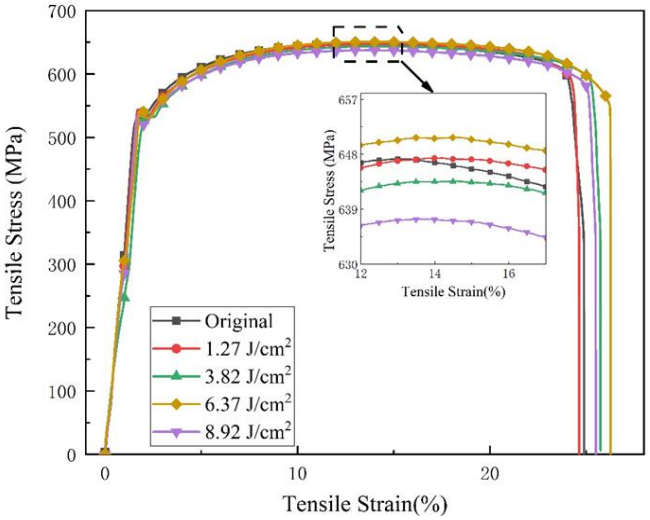

Fig. 8. Stress and strain curves of the before and after laser cleaning samples with different laser fluence at 70%.

IV. Conclusion

(1) Nanosecond pulsed laser cleaning of titanium alloys has a remarkable effect. Laser cleaning process were conducted using laser fluence and spot overlap ratio as variables. The optimal process parameters were spot overlap ratio 70% and the laser fluence 6.37 J/cm^2.

(2) The oxide film removal process exhibits sequential stages with increasing laser fluence: incomplete cleaning, partial cleaning, complete cleaning, and eventual substrate damage characterized by periodic ridge structure formation. Molten solidification marks appear on the cladding surface when the laser fluence exceeds 2.55 J/cm^2. The surface roughness first increases and then decreases with laser fluence increases.

(3) The higher laser fluence causes the substrate melting depth to increase, forming a periodic ridge structure with laser shock, plasma, gravity and molten substrate surface tension. These surface micro-nano structure can play an important role in the subsequent anti-deicing technology.

(4) Laser cleaning technology, when employing optimal parameters, enhances the tensile strength and strain characteristics of titanium alloys. The surface morphology is optimal with laser fluence 6.37 J/cm^2 and spot overlap ratio 70%, and the stress and strain are about 647 MPa and 26%, respectively. This is of great significance to the aviation manufacturing application of laser cleaning technology.

References

[1] X.Y. Liu, P.K. Chu, C.X. Ding, "Surface modification of titanium, titanium alloys, and related materials for biomedical applications", Materials Science & Engineering R-reports, vol.47, no.3-4, pp. 49-121, 2004.

[2] A.V. Yumashev, A.S. Utyuzh, M.V. Mikhailova, "Selecting clinical and laboratory methods of manufacture of orthopaedic titanium alloy structures using a biopotentiometer", Current Science, vol.114, no.4, pp. 891-896, 2018.

[3] M.M. Rasheedat, A. Esther, S. Mukul, P. Sisa, "Material Efficiency of Laser Metal Deposited Ti6Al4V: Effect of Laser Power", Engineering Letters, vol.21, no.1, pp. 18-22, 2013.

[4] K. Hiroyasu, T. Yoshimasa, I. Hideyuki, et al. "Application of titanium and titanium alloys to fixed dental prostheses", Journal of Prosthodontic Research, vol. 63, no.3, pp. 266-270, 2019.

[5] M. Izmir, B. Ercan, "Anodization of titanium alloys for orthopedic applications" Frontiers of Chemical Science and Engineering, vol. 13, no.1, pp. 28-45, 2019.

[6] V.S. Rudnev, V.P. Morozova, I.V. Lukiyanchuk, et al. "The Effect of Iron Precursors in an Electrolyte on the Formation, Composition, and Magnetic Properties of Oxide Coatings on Titanium", Nanoscale and Nanostructured Materials and Coatings, vol.53, no.6, pp. 1005-1014, 2017.

[7] P.S. Kishore, K. Rajnish, V.N. Vamsi, "Comparative study of mechanical and chemical methods for surface cleaning of a marine shell-and-tube heat exchanger", Heat Transfer-Asian Research, vol. 47, no.3, pp. 520-530, 2018.

[8] I. Alemzadeha, S. Nejatib, M. Vossoughic. "Removal of Phenols from Wastewater with Encapsulated Horseradish Peroxidase in Calcium Alginate", Engineering Letters, vol. 17, no.4, pp. 297-300, 2009.

[9] E. Fuchs, S. Kricke, E. Schohl, et al. "Effect of industrial scale stand-off distance on water jet break-up, cleaning and forces imposed on soil layers", Food and Bioproducts Processing, vol. 113, pp. 129-141, 2019.

[10] M.K.A.A. Razab, Noor A. Mohamed, Jaafar M. Suhaimi, et al. "A review of incorporating Nd:YAG laser cleaning principal in automotive industry", J Radiat Res Appl Sci, vol.11, no. 4, pp. 393-402, 2018.

[11] V. Gomes, A. Dionisio, J.S. Pozo-Antonio, "Mechanical and laser cleaning of spray graffiti paints on a granite subjected to a SO_2-rich atmosphere", Constr. Build. Mater, vol.188, pp. 621-632, 2018.

[12] X.L. Liu, Y.Q. Xiong, N. Ren, "Theoretical model for ablation of thick aluminum film on polyimide substrate by laser etching", J. Laser. Appl., vol. 30, no.4, pp. 1-7, 2018.

[13] M.W. Turner, M.J.J. Schmidt, L. Li, "Preliminary study into the effects of YAG laser processing of titanium 6Al– 4V alloy for potential aerospace component cleaning application", Appl Surf Sci, vol. 247, no.1-4, pp. 623-630, 2005.

[14] M.W. Turner, P.L. Crouse, L. Li, "Comparison of mechanisms and effects of Nd:YAG and CO_2 laser cleaning of titanium alloys", Appl Surf Sci, vol. 252, no. 13, pp. 4792-4797, 2006.

[15] M.W. Turner, P.L. Crouse, L. Li, et al. "Investigation into CO_2 laser cleaning of titanium alloys for gas-turbine component manufacture", Appl Surf Sci, vol. 252, no. 13, pp. 4798-4802, 2006.

[16] D.J. Whitehead, P.L. Crouse, M.J.J. Schmidt, et al. "Monitoring laser cleaning of titanium alloys by probe beam reflection and emission spectroscopy", Appl Phys A, vol. 93, pp. 123-127, 2008.

[17] L.Y. Yue, Z.B. Wang, L. Li, "Material morphological characteristics in laser ablation of alpha case from titanium alloy", Appl Surf Sci, vol. 258, no.20, pp. 8065-8071, 2012.

[18] B.W. Liu, G.Y. Mi, C.M. Wang, "Modification of TA15 alloy surface by high-pulse-frequency laser cleaning", J Laser Appl, vol. 32, no. 3, 032019, 2020.

[19] B.W. Liu, G.Y. Mi, C.M. Wang, "Research on grain refinement and wear behavior of micro-remelted Ta15 alloy surface by laser cleaning", Mater Chem and Physics, vol. 259, 124022, 2021.

[20] A. Kumar, M. Sapp, J. Vincelli, et al. "A study on laser cleaning and pulsed gas tungsten arc welding of Ti-3Al-2.5V alloy tubes", J Mater Process Tech, vol. 210, no. 1, pp. 64-71, 2010.

[21] Z.C. Li, D.H. Zhang, X. Su, et al., "Removal mechanism of surface cleaning on TA15 titanium alloy using nanosecond pulsed laser", Opt. & Laser Technol, vol. 139, 106998, 2021.

[22] Z.C. Li, J. Xu, D.H. Zhang, et al., "Nanosecond pulsed laser cleaning of titanium alloy oxide films: modeling and experiments", J. Manuf. Process, vol. 82, no. 1, pp. 665-677, 2022.